PHYSICAL REVIEW D **92,** 014021 (2015)

Diagrammatic computation of multi-Higgs processes at very high energies: Scaling $\log \sigma_n$ with MadGraph

Valentin V. Khoze*

Department of Physics, Institute for Particle Physics Phenomenology, Durham University, Durham DH1 3LE, United Kingdom

(Received 6 May 2015; published 17 July 2015)

At very high energies scattering amplitudes in a spontaneously broken gauge theory into multiparticle final states are known to grow factorially with the number of particles produced. Using simple scalar field theory models with and without the vacuum expectation value, we compute total cross sections with up to seven particles in the final state at the leading order in perturbation theory with MadGraph. By exploring the known scaling properties of the multiparticle rates with the number of particles, we determine from these the general n-point cross sections in the large-n limit. In the high-multiplicity regime we are considering, $n \gg 1$ and $\lambda n =$ fixed, the perturbation theory becomes strongly coupled with the higher-order loop effects contributing increasing powers of λn. In the approximation where only the leading loop effects are included, we show that the corresponding perturbative cross sections grow exponentially and ultimately violate perturbative unitarity. This occurs at surprisingly low energy scales ~40–50 TeV with multiplicities above ~150. It is expected that a repair mechanism or an extension of the theory has to set-in before these scales are reached, possibly involving a novel nonperturbative dynamics in the *a priori* weakly coupled theory.

DOI: 10.1103/PhysRevD.92.014021 PACS numbers: 12.38.Bx, 11.15.Bt

I. INTRODUCTION

We are interested in scattering processes at very high energies into n-particle final states in the limit $n \gg 1$. In this case the well-known problem of divergences of *large* orders of perturbation theory [1–4], is realized instead at the *leading* order. This is because even the leading-order Born diagrams for the n-point scattering amplitudes are expressed in terms of Feynman diagrams with large numbers of vertices, and with the numbers of diagrams growing factorially with n. At sufficiently high energies the production of high multiplicity final states, with n greater than the inverse coupling constant, is kinematically allowed and the n-point scattering amplitudes near the multiparticle mass thresholds grow as $n!$ at leading order, i.e. tree level in a weakly coupled theory.

In the simplest scenarios, production rates for such final states can be considered in a quantum field theory with a single scalar field of mass M and the coupling λ. The model with a nonvanishing vacuum expectation value $\langle h \rangle = v$,

$$\mathcal{L}^{\rm SSB} = \frac{1}{2}\partial^\mu h \partial_\mu h - \frac{\lambda}{4}(h^2 - v^2)^2, \qquad (1.1)$$

is a simplified version of the Higgs sector of the Standard Model (SM) in the unitary gauge, describing neutral Higgs bosons of mass $M = \sqrt{2\lambda}v$. We will refer to this model as the theory with spontaneous symmetry breaking (SSB), and it will be our principal case of interest for this paper. In addition to (1.1) we will also consider multiparticle amplitudes in an even simpler ϕ^4 theory, with no spontaneous symmetry breaking,

$$\mathcal{L}^{\text{no SSB}} = \frac{1}{2}(\partial\phi)^2 - \frac{1}{2}M^2\phi^2 - \frac{1}{4}\lambda\phi^4. \qquad (1.2)$$

The model (1.2) with an unbroken $\mathcal{Z}_2$ symmetry was widely used in computations of multiparticle rates in the 1990s as reviewed in Ref. [5] and other papers referenced therein and below.

Our goal here is to compute the multiparticle rates directly in perturbation theory using one of the current state-of-the-art publicly available numerical techniques, in the this case, MadGraph 5 [6]. The continuation procedure from moderate values of $n = 7$ particles in the final state, where our calculations are performed, to the regime with $n \sim 10^2$–10^3 will be set up and carried out in Sec. III based on the known scaling properties of the multiparticle cross sections with n, as will be outlined next in Sec. II.

II. MULTIPARTICLE PRODUCTION RATES AND THE HOLY GRAIL FUNCTION

Let us consider the multiparticle limit $n \gg 1$ for the n-particle final states and scale the energy $\sqrt{s} = E$ linearly with n, $E \propto n$, keeping the coupling constant small at the same time, $\lambda \propto 1/n$. It was first argued in [7] (for a review of subsequent developments see [5]) that in this double-scaling limit, the production cross sections σ_n have a characteristic exponential form,

*valya.khoze@durham.ac.uk

$$\sigma_n \sim e^{nF(\lambda n,\varepsilon)}, \quad \text{for } n \to \infty, \qquad \lambda n = \text{fixed}, \quad \varepsilon = \text{fixed}, \tag{2.1}$$

where ε is the average kinetic energy per particle per mass in the final state,

$$\varepsilon = (E - nM)/(nM), \tag{2.2}$$

and $F(\lambda n, \varepsilon)$ is a certain *a priori* unknown function of two arguments. $F(\lambda n, \varepsilon)$ is often referred to as the "holy grail" function for the multiparticle production[1] in the perturbative sector.

At small values of ϵ and λn, the large-n behavior in (2.1) has been verified explicitly and the function $F(\lambda n, \epsilon)$ was computed in [7] for the VEV-less scalar theory (1.2), and later in [8] for the theory with the VEV (1.2) and more generally in a gauge-Higgs theory. These computations were carried out in perturbation theory at tree level combined with the simplifications arising in the nonrelativistic limit $\varepsilon \ll 1$ for the final-state particles. This approach has allowed for the analytic derivation of the corresponding tree-level amplitudes and their phase-space integration for all values of $n \gg 1$. It was found that the dependence of the holy grail function on its two arguments, λn and ε, factorizes into individual functions of each argument

$$\log \sigma_n^{\text{tree}}|_{n\to\infty} \to nF^{\text{tree}}(\lambda n, \varepsilon) = n(f_0(\lambda n) + f(\varepsilon)), \tag{2.3}$$

and the two independent functions are given by the following expressions in the model (1.2) of Ref. [7]:

$$f_0(\lambda n)^{\text{no SSB}} = \log\left(\frac{\lambda n}{16}\right) - 1, \qquad n = \text{odd}, \tag{2.4}$$

$$f(\varepsilon)^{\text{no SSB}}|_{\varepsilon\to 0} \to f(\varepsilon)_{\text{asympt}} = \frac{3}{2}\left(\log\left(\frac{\varepsilon}{3\pi}\right) + 1\right) - \frac{17}{12}\varepsilon, \tag{2.5}$$

and in the Higgs model (1.1) of Ref. [8], respectively,

$$f_0(\lambda n)^{\text{SSB}} = \log\left(\frac{\lambda n}{4}\right) - 1, \tag{2.6}$$

$$f(\varepsilon)^{\text{SSB}}|_{\varepsilon\to 0} \to f(\varepsilon)_{\text{asympt}} = \frac{3}{2}\left(\log\left(\frac{\varepsilon}{3\pi}\right) + 1\right) - \frac{25}{12}\varepsilon. \tag{2.7}$$

These results arise from integrating the known expressions [7,8] for the tree-level amplitudes near the multiparticle thresholds,

$$\mathcal{A}_{1^*\to n}^{\text{no SSB}} = n!\left(\frac{\lambda}{8M^2}\right)^{\frac{n-1}{2}} \exp\left[-\frac{5}{6}n\varepsilon\right], \tag{2.8}$$

$$\mathcal{A}_{1^*\to n}^{\text{SSB}} = n!\left(\frac{\lambda}{2M^2}\right)^{\frac{n-1}{2}} \exp\left[-\frac{7}{6}n\varepsilon\right], \tag{2.9}$$

over the Lorentz-invariant phase space, $\sigma_n = \frac{1}{n!}\int \Phi_n |\mathcal{A}_n|^2$, in the large-$n$ nonrelativistic approximation. In particular, the ubiquitous factorial growth of the large-n amplitudes in (2.8)–(2.9) translates into the $\frac{1}{n!}|\mathcal{A}_n|^2 \sim n!\lambda^n \sim e^{n\log(\lambda n)}$ factor in the cross section, which determines the function $f_0(\lambda n)$ in (2.4) and (2.6). The energy dependence of the cross section is dictated by $f(\varepsilon)$ in Eq. (2.1), and this function arises from integrating the ε-dependent factors in (2.8)–(2.9) over the phase space, giving rise to the small-ε asymptotics in (2.5) and (2.7).

For our forthcoming analysis, an important point to make is that the separability or factorization of the λn from the ε dependence on the right-hand side of Eq. (2.1) is the general consequence of the tree-level approach; i.e. it does not require taking the nonrelativistic limit $\varepsilon \ll 1$. This is because the entire λ dependence of the full tree-level result $\sigma_n \propto \lambda^n$ is contained in the f_0 function. Hence, given that the dependence on n could enter $f(\varepsilon)$ only in the combination λn and that the dependence on λ is already fully accounted for,[2] the function $f(\varepsilon)$ does not depend on n. We, thus, should be able to determine $f(\varepsilon)$ from the fixed-n direct calculations of the cross sections, and using the large-n scaling arguments suggested by (2.1). In Sec. III we proceed to construct $f(\varepsilon)$ from the cross-section data at $n = 7$ which will be computed numerically using MadGraph [6].

It should also be kept in mind that the holy grail function in the cross-section formula Eq. (2.1) contains not only the tree-level contributions but also the loop contributions with an arbitrary number of loops, which to a large extent give the dominant contributions for $\lambda n \gtrsim 1$, as will be explored in more detail below.

III. RESULTS

With MadGraph 5 [6] we can compute quite efficiently total cross sections for scattering processes with $2 \to 7$ particles. As we are mainly interested in producing the multiparticle final state, we can make certain simplifications with respect to the characterization of the initial two-particle state. First, we take that the scattering process proceeds originates from the gluon fusion in the initial state, producing the highly virtual single Higgs boson h^* via the effective ggh vertex $\frac{\alpha_s}{12\pi v} h \text{tr} G^{\mu\nu} G_{\mu\nu}$, which is followed by the $1^* \to n$ process computed in the scalar theory (1.1) or (1.2),

[1] Equation (2.1) can be equivalently written in the form [7] $\sigma_n \sim \exp[\lambda^{-1}\mathcal{F}(\lambda n, \epsilon)]$, using the rescaling $\mathcal{F}(\lambda n, \epsilon) = \lambda n F(\lambda n, \varepsilon)$, which points towards a semiclassical interpretation of the rate in the $\lambda \to 0$ limit.

[2] We recall that this argument applies at tree level.

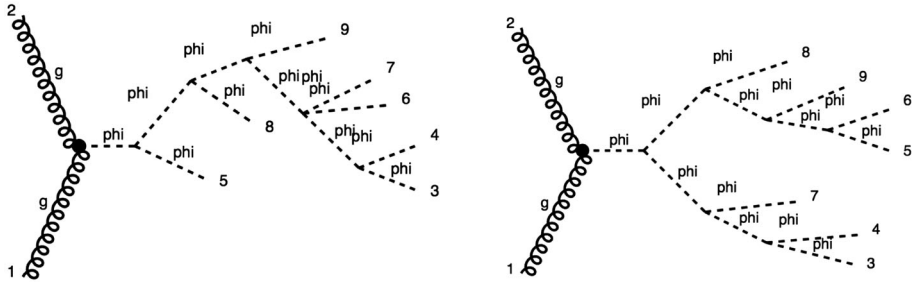

FIG. 1. Representative Feynman diagrams for the $gg \to 7h$ process in the SSB theory (1.1).

$$gg \to h^* \to n \times h. \tag{3.1}$$

In principle, as is well known, the use of the pointlike effective ggh coupling approximation is not justified at high energies for producing realistic cross sections. Finite top mass effects in loop will result in the form factor in front of the exponential factor in the cross section. However, in our case the single effective vertex is only a gimmick—in practice we will be computing *ratios* of the cross sections at the same values of energy for different n. These ratios are insensitive to the bad high-energy behavior of the effective vertex in the initial state. In our final results plotted in Fig. 6 we will include the effect of the Higgs form factor, as shown in Eq. (3.12).

At $n = 7$ in the Higgs theory with SSB (1.1) MadGraph computes 34,300 diagrams (two of which are shown in Fig. 1) contributing to the tree-level scattering amplitude. The cross section values $\sigma_7^{\rm SSB}$ were then computed for different energies on a grid of ∼30 points with values of $\varepsilon = E/(7M) - 1$ ranging from 0.001 (nearly at the multiparticle threshold) to 250 (ultrarelativistic final state). We have chosen $M = 125$ GeV and set $\lambda = 1$.[3] To give an example, at $\varepsilon = 1$ which corresponds to 1750 GeV, the rate is $\sigma_7^{\rm SSB} = 8.913 \times 10^{-11} \pm 2.74 \times 10^{-13}$ pb, and at $\varepsilon = 30$ corresponding to 27125 GeV, the rate is $\sigma_7^{\rm SSB} = 2.818 \times 10^{-10} \pm 9.02 \times 10^{-13}$ pb. More data points for $\sigma_7^{\rm SSB}$ for $0.1 \le \varepsilon \le 250$ are shown in Fig. 2 as the upper contour (in blue).

A. Extracting $f(\varepsilon)$ from computed cross sections

The expression in (2.3) contains only the contributions growing with n; it does not include subleading corrections, and is valid, as it stands, only in the $n \to \infty$ limit. To be able to work at moderately large values of n, such as $n = 6, 7$, we now generalize this by including the subleading corrections in n. In general, they are of the form $\mathcal{O}(\log n)$ and $\mathcal{O}(n^0)$, so that in total we have

$$\log \sigma_n^{\rm tree} = n(f_0(\lambda n) + f(\varepsilon)) + c_0 \log n + c_1 f_1(\varepsilon) + c_2 + \mathcal{O}(1/n). \tag{3.2}$$

Here c_0, c_1 and c_2 are some unknown constants, and $f_1(\varepsilon)$ is a new function of the kinetic energy. For example, by carrying out the phase-space integration of the nonrelativistic amplitudes in the small-ε limit beyond the leading order in n one finds

$$\log \sigma_n^{\rm tree} \to n(f_0(\lambda n) + (3/2)\log \varepsilon) + c_0 \log n - (5/2)\log \varepsilon + c_2 + \mathcal{O}(1/n).$$

Returning to Eq. (3.2) we now consider the difference between the rates at n and $n-1$. This allows us to extract $f(\varepsilon)$ directly from the $\log \sigma_n - \log \sigma_{n-1}$ data as follows:

$$f(\varepsilon) = \log \sigma_n - \log \sigma_{n-1} - \left[n f_0(\lambda n) - (n-1) f_0(\lambda(n-1)) + 0.5 \log \frac{n}{n-1} \right]. \tag{3.3}$$

The main point is that the expression in square brackets is known as it is dictated by the known function $f_0(\lambda n)$ in (2.6). (In addition, the constant $c_0 = 0.5$ is fitted from the data, and it results in a small correction numerically.) Equation (3.3) is our main tool for computing the holy grail function in the model with SSB from the ratios of cross-section data for $n = 7$ and $n = 6$ particles in the final state.

The scattering amplitude into the final state with $n = 6$ bosons in the model (1.1) contains 2,485 Feynman diagrams at tree level. This is still a large enough number of diagrams (to be in the regime of a "high-order" perturbation theory), so we can use the improved large-n subtraction formula (3.3). The cross sections $\sigma_6^{\rm SSB}$ are computed on the same ε grid as before. The characteristic value at $\varepsilon = 1$ is now $\sigma_6^{\rm SSB} = 1.77 \times 10^{-9}$ pb, and at $\varepsilon = 30$ the rate is 1.649×10^{-9} pb.

Our results for the function $f(\varepsilon)$ in the Higgs theory (1.1) derived form the numerical cross-section data using (3.3) with $n = 7$, are shown on the left plot in Fig. 3. This plot

[3]This can—and for the applications in plots in Figs. 5, 6 will be—rescaled to the physical value $\lambda \simeq 1/8$ using the fact that for each n, $\sigma_n^{\rm tree} \propto \lambda^{n-1}$.

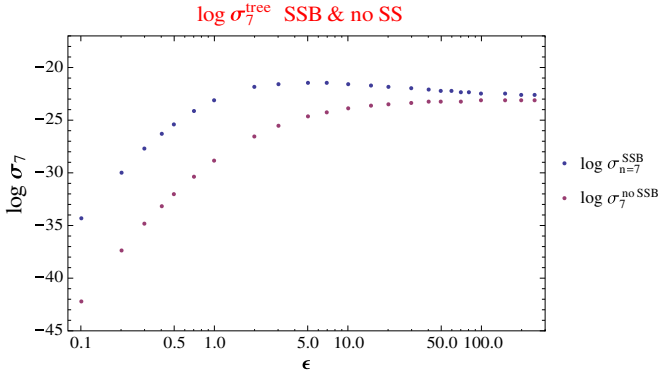

FIG. 2 (color online). Selection of data points for $\log\sigma_7$ as the function of ε computed with MadGraph in the models with and without spontaneous symmetry breaking (the upper and the lower contours).

also shows a perfect match to the known $f(\varepsilon)_{\text{asympt}}$ expression (2.7) at $\varepsilon < 1$, which is shown as a dashed curve in light blue. As another test of self-consistency of our procedure, we have checked that $f(\varepsilon)$ obtained from the 7–6 computation in fact matches closely the function extracted from a similar 6–5 computation.

For completeness, and to compare with the numerical predictions based on the semiclassical analysis in [5,9,10], we have also computed $f(\varepsilon)$ in the unbroken theory (1.2). Our results for $\sigma_7^{\text{n0 SSB}}$ for $0.1 \le \varepsilon \le 250$ are shown in Fig. 2 as the lower contour (in purple). The two values of the cross sections in the two models appear to converge in the UV. This is not surprising, since at very high energies, all mass parameters become irrelevant and there is little difference between the models with the "right" and the "wrong" sign of the mass-squared term.

To determine $f(\varepsilon)$ in the unbroken theory from the diagrammatic computation, we use the master formula,

$$2f(\varepsilon) = \log\sigma_n - \log\sigma_{n-2} - \left[nf_0(\lambda n) - (n-2)f_0(\lambda(n-2)) + 0.5\log\frac{n}{n-2}\right], \tag{3.4}$$

for the $n = 7$ and $n = 5$ rates (in the unbroken theory there are no three-point vertices and the amplitudes are nonvanishing only for odd values of n). Our results are shown on the right plot in Fig. 3. The left panel in Fig. 4 plots the results for $f(\varepsilon)$ functions in the SSB model and the unbroken theory side by side for moderate to large values of ε.

In principle, we should keep in mind that our analysis is based on the applicability of the subtraction formulas which assume that n is large enough to ensure that $1/n$ corrections are negligible in the subtraction formulas. Thus, our derivation of $f(\varepsilon)$ in the unbroken theory, which is based on the $n = 7$ and $n = 5$ data with (280 and 10 Feynman diagrams), is less robust in comparison to our main SSB theory results based on the $n = 7$ and $n = 6$ data with 34,330 and 2,485 Feynman diagrams. However, computations of $2 \to 9$ processes with MadGraph, which would be the next step in the unbroken theory, is beyond the scope of this paper.

B. Multiparticle cross sections

Having determined the n-independent kinetic energy function $f(\varepsilon)$ allows us to compute multiparticle cross sections at any n in the large-n limit. The tree-level multiparticle cross sections σ_n^{tree} in the scalar theory with SSB are obtained via

$$\log\sigma_n(E) = n(f_0(\lambda n) + f(\varepsilon)), \tag{3.5}$$

with $\varepsilon(E,n) = (E - nM)/(nM)$ and

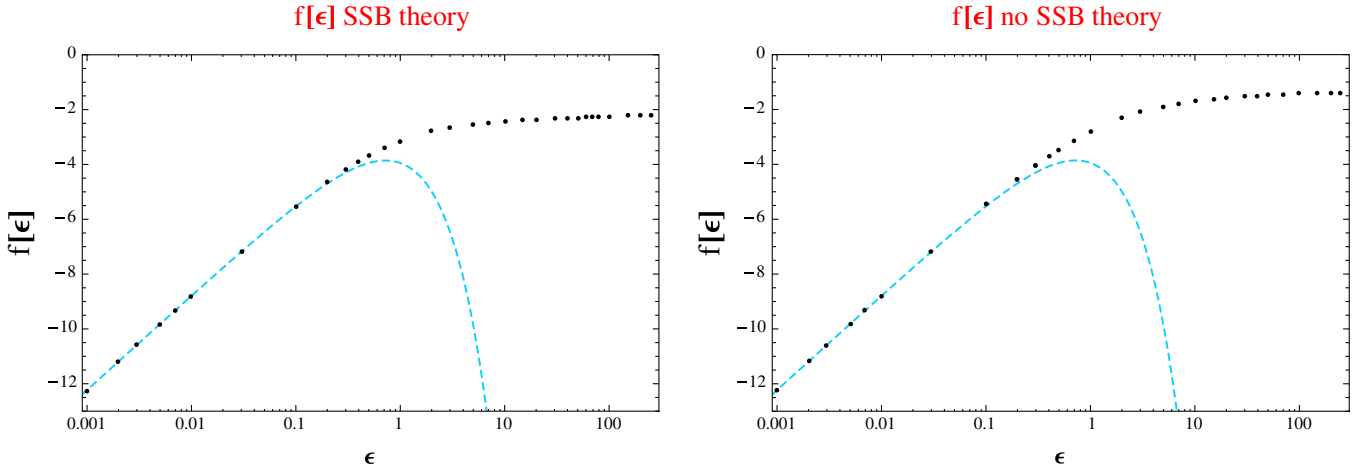

FIG. 3 (color online). Plots of $f(\varepsilon)$ extracted from the $\log\sigma_7^{\text{tree}}/\sigma_6^{\text{tree}}$ MadGraph data in the SSB model, and the $\log\sigma_7^{\text{tree}}/\sigma_5^{\text{tree}}$ realization of $f(\varepsilon)$ in the model without SSB. The results perfectly match $f(\varepsilon)_{\text{asympt}}$ for $\varepsilon < 1$ depicted in light blue.

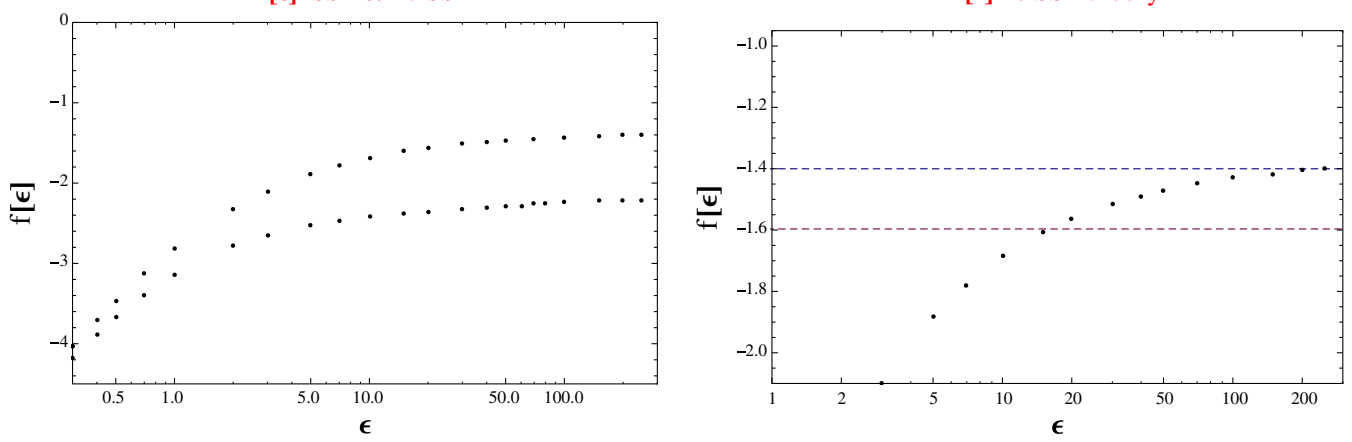

FIG. 4 (color online). Plots of $f(\varepsilon)$ in the broken and unbroken theory for medium to large values of ε. In the UV regime the functions asymptote to $f(\varepsilon = 250)^{\text{SSB}} \simeq -2.2$ and $f(\varepsilon = 250)^{\text{no SSB}} \simeq -1.4$. The plot on the right depicts $f(\varepsilon)^{\text{no SSB}}$ and shows that it exceeds the asymptotic lower limit $-\log \pi^2/2 \simeq -1.6$ obtained from the O(4) symmetric classical solution [5,9,10].

$$f_0(\lambda n)^{\text{SSB tree}} = \log\left(\frac{\lambda n}{4}\right) - 1, \tag{3.6}$$

and we set $\lambda = 1/8$ and $M = 125$ GeV. In Fig. 5 we plot the cross sections σ_n^{tree} in this theory as a function of energy E for a range of final-state multiplicities between $n = 1000$ and $n = 1500$. The choice of such high values of particles in the final state follows from selecting the regime where the tree-level cross sections become unsuppressed. This occurs when the positive $f_0(\lambda n)^{\text{SSB tree}}$ factor is able to compensate the negative values of $f(\varepsilon)$. As a result, we see that perturbative cross sections grow very steeply with energy, and the interesting range of energies where the $\log \sigma_n^{\text{tree}}$ crosses zero occurs is the $E \sim 500$ TeV regime. At these energies the tree-level cross sections grow exponentially violating perturbative unitarity. The energy regime where this happens in Fig. 5 is in agreement with the estimates obtained in [11]. What is interesting is that the energy scales where perturbation theory breaks down (judging from the leading tree-level analysis here) occur at energies only a (few) $\times 10^1$ above what could be directly tested experimentally with a hadron Future Circular Collider (FCC) collider.

Let us now consider the effect of loop corrections. The one-loop corrected multiparticle amplitudes on multiparticle thresholds are known [12,13], and the result in the broken scalar theory (1.1) is given by [13]

$$\text{SSB}: \mathcal{A}_{1^*\to n}^{\text{tree+1 loop}} = n!(2v)^{1-n}\left(1 + n(n-1)\frac{\sqrt{3}\lambda}{8\pi}\right). \tag{3.7}$$

It was shown in Ref. [7], based on the analysis of leading singularities of the multiloop expansion around singular generating functions in scalar field theory, that the one-loop correction exponentiates,

$$\mathcal{A}_{1^*\to n}^{\text{loops}} = \mathcal{A}_{1^*\to n}^{\text{tree}} \times \exp\left[B\lambda n^2 + \mathcal{O}(\lambda n)\right], \tag{3.8}$$

in the limit $\lambda \to 0$, $n \to \infty$ with λn^2 fixed, where B is the constant factor determined from the one-loop calculation,

$$\text{model with SSB (1.1)}: B = +\frac{\sqrt{3}}{8\pi}, \tag{3.9}$$

$$\text{unbroken model (1.2)}: B = -\frac{1}{64\pi^2}(\log(7 + 4\sqrt{3}) - i\pi). \tag{3.10}$$

As a result, the leading-order multiloop exponentiation leads to the exponential enhancement of the multiparticle cross section in the Higgs model, cf. Eqs. (2.6) and (3.14),

$$f_0(\lambda n)^{\text{loop}} = \log\left(\frac{\lambda n}{4}\right) - 1 + 2B\lambda n. \tag{3.11}$$

Finally we can also include the single Higgs production form factor in front of the exponential factor in the cross section, to correct for our use of the effective Higgs-gluon vertex in the large energy limit,[4]

$$\sigma_n^{\text{loop}} = (m_t/E)^4 \log^4(m_t/E)^2 e^{n(f_0(\lambda n)+f(\varepsilon))}, \tag{3.12}$$

where m_t is the top mass. In total we have

$$\log \sigma_n^{\text{loop}} = n(f_0(\lambda n)^{\text{loop}} + f(\varepsilon)) - 4(\log(E/m_t) - \log\log(E^2/m_t^2)), \tag{3.13}$$

$$f_0(\lambda n)^{\text{loop}} = \log\left(\frac{\lambda n}{4}\right) - 1 + \sqrt{3}\frac{\lambda n}{4\pi}, \tag{3.14}$$

[4]I would like to thank Michael Spira for this suggestion.

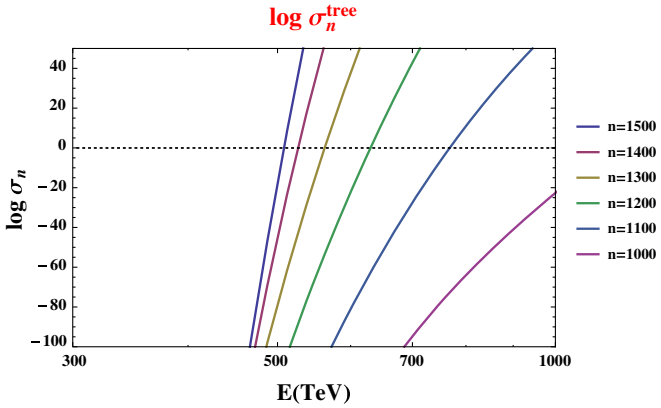

FIG. 5 (color online). Plots of multiparticle tree-level cross sections σ_n^{tree} in the scalar model with SSB as the function of energy E for a range of final-state multiplicities between $n = 1000$ and $n = 1500$.

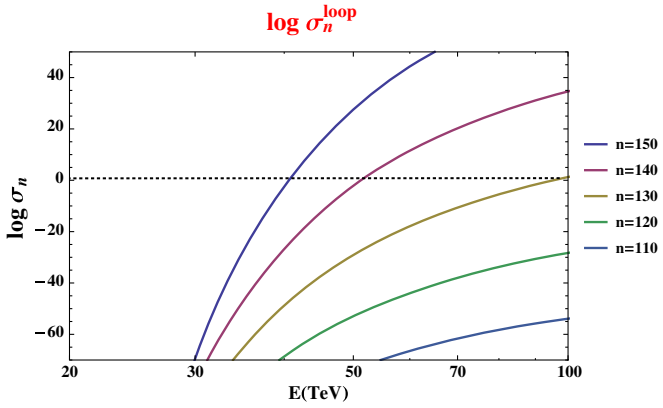

FIG. 6 (color online). Results for multiparticle cross sections σ_n^{loop} with the leading-loop-resummation factor (3.13)–(3.14) and the single Higgs production form facror in the model with SSB (1.1). The logarithm of the cross section (3.12) is plotted as the function of energy for a range of final-state multiplicities between $n = 110$ and $n = 150$.

where the last equation is consistent with (3.9) and leads to the exponential enhancement of the cross section σ_n, at least in the leading order in $n^2\lambda$. The form-factor correction—the last term on the right-hand side of (3.13)—grows with n only logarithmically[5] compared to the linear in n terms in the first term. (At $E = 50$ TeV the form factor gives the correction $-4(\log(E/m_t) - \log\log(E^2/m_t^2)) \simeq -12.95$ in the exponent.)

Our results for σ_n^{loop} including the form factor and the exponentiated loop factor [the last term in (3.14)] for the Higgs model (1.1) are shown in Fig. 6 for a range of final-state multiplicities between $n = 110$ and $n = 150$. We can see that the loop enhancement has reduced the energy scale (and multiplicities) by a factor of 10, and the scale for the perturbation theory breakdown or equivalently the scale of new phenomena to set in is now reduced to 40–50 TeV which is pretty much within the energy reach of the 100 TeV FCC collider, in agreement with the estimate in [11].

Of course, one should keep in mind that the setup in Eqs. (3.13)–(3.14) is merely an optimistic phenomenological model. In general, the even higher-order effects of loop exponentiation will be present such that

$$f_0(\lambda n)^{\text{all loops}} = \log\left(\frac{\lambda n}{4}\right) - 1 + \sqrt{3}\frac{\lambda n}{4\pi} + \text{const}\left(\frac{\lambda n}{4\pi}\right)^2 + \text{const}'\left(\frac{\lambda n}{4\pi}\right)^3 + \cdots \tag{3.15}$$

and can change the cross-section contours in Fig. 6. (Note that the values of the loop expansion parameter $\frac{\lambda n}{4\pi}$ are $\simeq 1$ for $n = 100$ and $\simeq 1.4$ for $n = 140$.)

[5]At large n and large ε limit, it is $\simeq -4\log(n\varepsilon) + 4\log\log(n\varepsilon) + 4\log((m_t/M)\log(M/m_t))$.

IV. CONCLUSIONS

Our diagrammatic approach is conceptually different (but also complimentary) to the semiclassical considerations followed in the earlier literature. The exponential form of the cross section in the large-n limit,

$$\sigma_n \sim \exp\left[\frac{1}{\lambda}\lambda n F(\lambda n, \epsilon)\right] := \exp\left[\frac{1}{\lambda}\mathcal{F}(\lambda n, \epsilon)\right], \tag{4.1}$$

is strongly suggestive of an underlying semiclassical origin of the multiparticle cross section. In particular, there is a strong similarity between the purely perturbative multiparticle processes considered here and the $B + L$-violating nonperturbative reactions in the instanton sector of the SM discussed originally in [14].

The idea that semiclassical methods can be also used in the perturbative sector of the theory was put forward and explored by a number of authors including Refs. [5,9,10,15,16]. At tree level the holy grail function F or $\mathcal{F}$ can indeed be reconstructed numerically if one can determine certain singular classical solutions to the boundary value problem [9], as explained in [5,9,10]. In practice, this procedure was carried out in the case of the unbroken ϕ^4 theory (1.2) and based on finding numerically the singular solutions with the hypothesized O(4) symmetry. In this approach, a lower bound on the tree-level cross section (2.1) was derived in [5,10] which corresponds to an upper bound on the absolute value of $|f(\varepsilon)|$. In particular, it was found that at infinite energies, $\varepsilon \to \infty$ the function $f(\varepsilon) \to -\log(\pi^2/2) \simeq -1.6$. In our case, the asymptotic value appears to be smaller in magnitude in the non-SSB theory, $f(\varepsilon) \to -1.6$, as can be seen from the right panel in Fig. 4. The fact that $f(\varepsilon) \to -|\text{const}|$ implies

$$\sigma_n^{\text{tree noSSB}} \gtrsim e^{-|\text{const}|n} e^{n f_0(\lambda n)} \quad \text{at } E \to \infty. \tag{4.2}$$

An often quoted misreading of this result is the statement that perturbative cross sections remain unobservable in the multiparticle limit, even at infinitely high energies, due to a rising with n exponential suppression factor $e^{-|\text{const}|n}$. This, of course, is not the case as the plots in Figs. 5 and 6 demonstrate: the growing function $e^{nf_0(\lambda n)}$ compensates the suppression in $e^{-|\text{const}|n}$ for any ε already at moderately high values of λn.

One advantage of the diagrammatic approach followed in this paper is its simplicity and also the fact that one should be able to apply it in any theory, ultimately including the full gauge-Higgs theory of the SM weak sector by generalizing the nonrelativistic results of [8,17] to the general-ε case. We leave this to future work.

Since in our case the calculations are carried out within the first principles perturbative approach, we also know that as soon as the regime is reached where the theory breaks down and violates unitarity, this implies that we really are falsifying the perturbative technique itself, and not a bound arising from a semiclassical treatment. The perturbation theory breakdown found here occurs in two cases: (a) within the tree-level approximation in the energy-multiplicity regime of Fig. 5 and (b) within the leading order in the loop expansion approximation in the regime corresponding to Fig. 6.

To what extent do our results rely on accepting the exponentiated form of the high-multiplicity cross section (2.1) as an input? Equation (2.1), after all, is a conjecture [5,7]. However, we know that at tree level the corresponding equation (2.3) does agree with the analytic expressions in (2.4)–(2.5) or (2.6)–(2.7) derived in perturbation theory in the nonrelativistic limit $\varepsilon \to 0$. This agreement is manifest in both plots in Figure 3 which show that the data points at $\varepsilon \lesssim 1$ are on top of the dashed lines representing the first-principles analytic expressions in the nonrelativistic limit. Furthermore, as we pointed out in the closing paragraphs of Sec. II, the factorization of the λn-from the ε dependence on the right-hand side of Eq. (2.1), which served as the basis of the subtraction formula (3.3) used to define the energy-dependent part $f(\varepsilon)$, is the general consequence of the tree-level approach and does not require the nonrelativistic limit. Hence, at tree level our results in Fig. 3 can be seen as providing additional evidence for the exponentiated form (2.1). At loop level, however, we are strongly relying on the exponentiated form of the cross section as an input, and in particular, the exponentiation of the leading-loop-order correction computed on threshold—specifically the last term on the right-hand side of Eq. (3.11). Our actual predictions of the energy scales and particle multiplicities where these process can become unsuppressed and ultimately lead to the perturbation theory breakdown, cf. Fig. 5 for tree-level processes and Fig. 6 which assumes the dominance of the leading-loop exponentiation effect, are, as we have already explained, a combination of the direct diagrammatic computations at moderately high multiplicities, scaled to the very high-multiplicity values using the ansatz dictated by the exponentiated form of the cross section.

The main technical challenge which still needs to be addressed is how to account for all the remaining higher-loop corrections, relevant in the regime $\lambda n \sim 1$. Even the leading-order exponentiation of the loop corrections result (the last term on the right-hand side of [(3.14)] which was essential for lowering the characteristic energy scale from Fig. 5 to Fig. 6 by an order of magnitude, has been derived only in the multiparticle threshold limit; the full ε dependence of leading-loop corrections remains unknown.

Another (perhaps less crucial) technical limitation of our simple derivation is that we have concentrated only on subprocesses with a single virtual Higgs in the s channel in (3.1). We have not considered here the effect of possible numerical partial cancellations between the s-channel $\bar{t} \to h^* \to hh$ and box diagram processes $\bar{t} \to hh$ and in the double Higgs case and generalizations for the multi-Higgs case, see e.g. the discussion in [18]. However, in the absence of the symmetry reason, we do not expect that such partial cancellations could significantly modify the exponential growth of the s-channel processes (3.1). This conclusion is also in agreement with the discussion in Sec. 4 of [11] where we have seen that the exponential growth persists in the similar case of the weak vector boson fusion, $VV \to h^* \to hh \to n \times h$ vs $VV \to h^*h^* \to n \times h$.

We have shown that in very high-energy scattering events, perturbative rates for production of multiple Higgs bosons grow with increasing energy, eventually violating perturbative unitarity and resulting in the breakdown of the ordinary weakly coupled perturbation theory. The energy scales where electroweak processes can enter this regime are potentially within the reach of the 100 TeV future hadron colliders, or at least not much above it. It was argued in [11] that novel physics phenomena must set in before these energies are reached: either the electroweak sector becomes nonperturbative in this regime, or additional physics beyond the SM might be needed.

ACKNOWLEDGMENTS

I am grateful to Joerg Jaeckel, Michelangelo Mangano, Gavin Salam and Michael Spira for discussions and comments about computing multiparticle rates from first principles at finite n, and to Olivier Mattelaer and Gunnar Ro for sharing with me their expertise with MadGraph. This work is supported by the STFC through the IPPP grant and by the Royal Society Wolfson Research Merit Award.

[1] F. J. Dyson, Divergence of perturbation theory in quantum electrodynamics, Phys. Rev. **85**, 631 (1952).
[2] L. N. Lipatov, Divergence of the perturbation theory series and the quasiclassical theory, Sov. Phys. JETP **45**, 216 (1977) [Zh. Eksp. Teor. Fiz. **72**, 411 (1977)].
[3] E. Brezin, J. C. Le Guillou, and J. Zinn-Justin, Perturbation theory at large order. 1. The φ^{2N} interaction, Phys. Rev. D **15**, 1544 (1977).
[4] G. 't Hooft, Can we make sense out of quantum chromodynamics?, Subnucl. Ser. **15**, 943 (1979); Under the spell of the gauge principle, Adv. Ser. Math. Phys. **19**, 1 (1994).
[5] M. V. Libanov, V. A. Rubakov, and S. V. Troitsky, Multiparticle processes and semiclassical analysis in bosonic field theories, Phys. Part. Nucl. **28**, 217 (1997).
[6] J. Alwall, M. Herquet, F. Maltoni, O. Mattelaer, and T. Stelzer, MadGraph 5: Going beyond, J. High Energy Phys. 06 (2011) 128.
[7] M. V. Libanov, V. A. Rubakov, D. T. Son, and S. V. Troitsky, Exponentiation of multiparticle amplitudes in scalar theories, Phys. Rev. D **50**, 7553 (1994).
[8] V. V. Khoze, Perturbative growth of high-multiplicity W, Z and Higgs production processes at high energies, J. High Energy Phys. 03 (2015) 038.
[9] D. T. Son, Semiclassical approach for multiparticle production in scalar theories, Nucl. Phys. **B477**, 378 (1996).
[10] F. L. Bezrukov, M. V. Libanov, D. T. Son, and S. V. Troitsky, Singular classical solutions and tree multiparticle cross-sections in scalar theories, in *Zvenigorod 1995, High Energy Physics and Quantum Field Theory*, p. 228.
[11] J. Jaeckel and V. V. Khoze, An upper limit on the scale of new physics phenomena from rising cross sections in high multiplicity Higgs and vector boson events, Phys. Rev. D **91**, 093007 (2015).
[12] M. B. Voloshin, Summing one loop graphs at multiparticle threshold, Phys. Rev. D **47**, R357 (1993).
[13] B. H. Smith, Summing one loop graphs in a theory with broken symmetry, Phys. Rev. D **47**, 3518 (1993).
[14] A. Ringwald, High-energy breakdown of perturbation theory in the electroweak instanton sector, Nucl. Phys. **B330**, 1 (1990); L. G. Yaffe, Report No. DOE-ER-40423-PT-90-07, C90-04-27 (Santa Fe SSC Workshop, 1990); P. B. Arnold and M. P. Mattis, Baryon violation at the SSC? Recent claims reexamined, Phys. Rev. D **42**, 1738 (1990); S. Y. Khlebnikov, V. A. Rubakov, and P. G. Tinyakov, Instanton induced cross-sections below the sphaleron, Nucl. Phys. **B350**, 441 (1991); A. H. Mueller, Leading power corrections to the semiclassical approximation for gauge meson collisions in the one instanton sector, Nucl. Phys. **B353**, 44 (1991); V. V. Khoze and A. Ringwald, Total cross-section for anomalous fermion number violation via dispersion relation, Nucl. Phys. **B355**, 351 (1991); Nonperturbative contribution to total cross-sections in nonAbelian gauge theories, Phys. Lett. B **259**, 106 (1991).
[15] M. B. Voloshin, On strong high-energy scattering in theories with weak coupling, Phys. Rev. D **43**, 1726 (1991).
[16] A. S. Gorsky and M. B. Voloshin, Nonperturbative production of multiboson states and quantum bubbles, Phys. Rev. D **48**, 3843 (1993).
[17] V. V. Khoze, Multiparticle Higgs and vector boson amplitudes at threshold, J. High Energy Phys. 07 (2014) 008.
[18] X. Li and M. B. Voloshin, Remarks on double Higgs boson production by gluon fusion at threshold, Phys. Rev. D **89**, 013012 (2014).